

COMBINING BRAIN IMAGING DATA WITH ELECTRONIC HEALTH RECORDS TO NON-INVASIVELY QUANTIFY [¹¹C]DASB BINDING

Arthur Mikhno¹, Francesca Zanderigo², R Todd Ogden⁵, Michelle Mikhno³, Harry Nagendra⁴,
J. John Mann⁵, Andrew F. Laine¹, Ramin V. Parsey²

1. Department of Biomedical Engineering, Columbia University, NY. 2. Department of Psychiatry, Stony Brook University, NY
3. Rutgers University, New Jersey. 4. SUNY Downstate Medical Center, New York. 5. Department of Psychiatry, Columbia University, NY

ABSTRACT

Quantitative analysis of PET data requires a metabolite-corrected arterial input function (AIF) for estimation of distribution volume and related outcome measures. Collecting arterial blood samples adds risk, cost, and patient discomfort to PET studies. Minimally invasive AIF estimation is possible with simultaneous estimation (SIME), but one arterial blood sample is necessary to be used as an anchor value to ensure identifiability of each individual's AIF. For [¹¹C]DASB, a widely used serotonin transporter PET tracer, this blood sample is optimally taken 50 minutes after injection. We present here an approach for replacing such a single time-point anchor with a predicted value using brain imaging and electronic health record (EHR) data. Average bootstrap $R^2 > 0.8$ in training data suggest that up to 80% of the variance in [¹¹C]DASB SIME anchor may be explained by a model including heart rate, blood pressure, tracer dose, body size and cerebellar gray matter uptake. Preliminary results show that these models generalize well to a small test dataset. This may allow for quantitative analysis with no blood sampling.

Index Terms— minimally/non-invasive PET, simultaneous estimation, image-derived input function

1. INTRODUCTION

Positron emission tomography (PET) is used for quantifying the distribution of receptors and proteins in the brain and the body. Quantitative analysis of PET data requires both the metabolite-corrected arterial input function (AIF) and the tissue time activity curves (TACs) derived from the image data for estimation of distribution volume and related outcome measures [1]. The AIF is measured in order to account for inter- and intra- individual variance in tracer availability due to metabolism and clearance. Blood samples are collected from the radial artery during the PET scan to calculate the AIF. This procedure adds risk, cost and patient discomfort to the demands of PET studies.

Significant progress has been made over the years towards less invasive PET analysis. Reference tissue methods have

been developed but require the existence of a reference region devoid of specific binding, which for [¹¹C]DASB does not exist [2]. Image-derived input function (IDIF) approaches recover the AIF by extracting signal from the carotid artery or cranial blood pools. IDIF methods are prone to partial volume effects and still require blood samples to scale the signal [3]. Minimally invasive AIF estimation is possible with simultaneous estimation (SIME) [4], but at least one blood sample still needed as an individual anchor value for identifiability. For [¹¹C]DASB, this sample is optimally taken 50 minutes after injection [4]. This single blood sample adds risk and discomfort to the study and leaves the PET analysis reliant on the accuracy of a single data point.

Population pharmacokinetics and pharmacodynamics (PPKD) is a field centered around predicting metabolite corrected blood levels of pharmaceutical compounds at various time points after injection/ingestion. This is done by aggregating blood data from multiple studies and searching for covariates (e.g. age, lab tests, etc.) that explain the variability in drug blood concentration [5]. As a PET tracer is also a pharmaceutical compound, similar covariate screening approaches may be effective for [¹¹C]DASB. PET imaging data may add additional information on tracer blood concentrations. Previous work suggests that combining supplementary information (e.g. weight, dose, etc.) with signal from cranial blood vessel improve prediction of the AIF [6]. However, this technique was developed with the [¹⁸F]FDG tracer, for which the AIF does not require metabolite correction, and thus the imaging data is highly correlated with the AIF. It is not clear if such an approach could translate to [¹¹C]DASB where the AIF profile is highly dependent on the rate of tracer metabolism and clearance.

In this study, we expand on [4, 5, 6] to combine [¹¹C]DASB brain imaging and electronic health record (EHR) data to develop a model for predicting the [¹¹C]DASB SIME anchor.

2. METHODOLOGY

2.1. Data collection

In this retrospective Institutional Review Board approved study, EHR and PET brain imaging data were gathered for

Male (N= 38), Female (N=57)			
Variable	Mean (STD)	min	max
Age (y)	38 (12)	19	64
Weight (lb)	165 (41)	102	279
Height (in)	66 (3)	60	73

Table 1: Descriptive Statistics

228 subjects who had undergone [^{11}C]DASB scans at The Kreitchman PET Center at Columbia University Medical Center from 2004 to 2012. EHR data collected prior to the PET scan date and included demographics (e.g., weight, gender, etc.), blood workup (e.g., chemistry, hematology, thyroid panel) and urinalysis (e.g., pH). PET data included sum 50-90 minute gray matter cerebellar activity (CER), injected dose (ID), injected mass, tracer specific activity, and the metabolite-corrected AIF. Heart rate (HR) and blood pressure (BP) were obtained within hours before and after the PET scan. Only subjects that had weight, height and AIF data available were included in the study. The final data set consisted of 95 subjects and 92 initial variables. Descriptive statistics for the subjects are shown in Table 1.

2.2. Heart rate and blood pressure

HR was measured manually via radial pulse rate before (HRpre) and after (HRpost) the PET scan. Systolic (SBP) and diastolic (DBP) BP measurements were obtained with a sphygmomanometer before (SBPpre, DBPpre) and after (SBPpost, DBPpost) the scan. HR and BP were manually transcribed from handwritten notes left on the PET protocol form by clinical technicians. Missing or illegible measurements were marked as NaN. Vitals were not assessed at consistent times, ranging between 9 and 1 hours for pre-scan and between 2 and 8 hours for post-scan measurements. Therefore, variables that represent the closest and average (avg) vitals were also calculated: HRclosest, SBPclosest, DBPclosest, HRavg, SBPavg, DBPavg. The following derived variables were also calculated based on HR and BP: mean arterial pressure (MAP), estimated cardiac output (eCO) and pulse pressure (PP), using Eq. 1-3. Summary statistics for vitals are shown in Table 2.

$$MAP = SBP + \frac{1}{3}(SBP - DBP) \quad (1)$$

$$PP = SBP - DBP \quad (2)$$

$$eCO = HR \times PP \quad (3)$$

2.3. Derived variables

Body-mass index (BMI) and surface area (BSA), estimated total blood volume (eTBV), estimated total plasma volume (eTPV), and estimated resting metabolic rate (eRMR) were

Variable	Mean (STD)	min	max
pre-scan Δt (h)	2.3 (1.2)	9	0.5
post-scan Δt (h)	4.9 (1.4)	1.9	7.8
SBPpre (mmHg)	122 (17)	90	189
DBPpre (mmHg)	75 (9)	53	107
HRpre (beats/min)	72 (11)	45	100
SBPpost	122 (17)	93	178
DBPpost	76 (12)	54	128
HRpost	73 (12)	48	105

Table 2: Vitals statistics

derived from the weight (W), height (H), and hematocrit (Hct):

$$BMI = 703 * W/H \quad (4)$$

$$BSA = \sqrt{(W * H)/3131} \quad (5)$$

$$eTBV = \begin{cases} 0.006012H^3 + 14.6W + 604, & \text{male} \\ 0.005835H^3 + 15.0W + 183, & \text{female} \end{cases} \quad (6)$$

$$eTPV = eTBV \times (1 - Hct) \quad (7)$$

$$eGFR = \begin{cases} 175Crt^{-1.154}Age^{-0.203}, & \text{male} \\ 129.85Crt^{-1.154}Age^{-0.203}, & \text{female} \end{cases} \quad (8)$$

$$eGFR_{BSA} = eGFR * BSA \quad (9)$$

The estimated glomerular filtration rate (eGFR) was calculated from the blood creatine level (Crt) as

$$eRMR = \begin{cases} 4.5W + 15.9H - 5Age + 5, & \text{male} \\ 4.5W + 15.9H - 5Age - 161, & \text{female} \end{cases} \quad (10)$$

Other calculated variables include osmolarity gap, albumin corrected calcium, blood viscosity, anion gap, BUN Creatine ratio, and plasma osmolarity using standard clinical formulas. Two additional variants of Eq. (9) were calculated using BUN and Albumin (GFR_5 , GFR_{5BSA}).

2.4. Variable selection

The combination of EHR, PET, demographics, vitals and derived variables amounted to 92 initial predictors, as shown in Table 3. Note that Total Plasma (TP) is the total radioactivity count in each blood sample taken at time t , where the $AIF(t) = ParentFraction(t) \times TP(t)$. For [^{11}C]DASB, the response variable is the SIME 50 minute anchor (SA50), or $SA50 = AIF(t = 50min)$. We took a multi-stage approach to screening variables that may be useful in predicting SA50. First, correlation with SA50 was examined, and variables retained if $R^2 > 0.1$. Second, new variables were created by normalizing each variable to the ID, as is done when calculating standardized uptake values. If the correlation of the ID/variable ratio and SA50 met the following criteria, $R^2 > R_{ID}^2 = 0.18$, then this new variable was retained

Initial Predictors (92)		
Chemistry (21)	Hematology (14)	LBMI
A/G Ratio	WBC	eTBV
Albumin	RBC	eTPV
Alk Phos	Hemoglobin	eGFR
ALT(SGPT)	Hematocrit	eGFR _{BSA}
AST(SGOT)	MCV	eGFR5
BUN	MCH	eGFR5 _{BSA}
Calcium	MCHC	RMR
Chloride	RDW	Osm gap
Cholesterol	Platelets	rCalcium
CO ₂	Neut Absolute	Blood viscosity
Creatinine	Lymph Absolute	Anion gap
Globulin	Mono Absolute	BUN:Crt ratio
Glucose	Eosin Absolute	Plas. Osm.
LDH	Baso Absolute	
Phosphorous	Urinalysis (3)	Vitals (24)
Potassium	Specific gravity	HR
Sodium	Urobilinogen	BP
T. Bilirubin	pH	MAP
Total Protein		PP
Triglyceride	Demographics(4)	eCO
Uric Acid	Weight	x2 (pre, post)
	Height	x2 (closest, avg)
Thyroid (5)	Age	
T3 Uptake	Sex	PET (4)
TSH		Cerebellar ROI
Thyroxine Free	Derived (16)	Injected Dose
Thyroxine Total	BMI	Injected Mass
Triiodothyronine	BSA	Specific Activity
		Total Plasma

Table 3: Initial Predictors

for further analysis. Finally, we conducted a search for two variable interaction terms. A total of 4186 (92 choose 2) multivariate regression models were evaluated, each consisting of two predictors with (mdl*) and without (mdl) an interaction term (*). If, $R_{mdl*}^2 > R_{mdl}^2$ AND $R_{mdl*}^2 > 0.1$ AND $p_* < 0.05$, the interaction term was retained as a prospective predictor.

2.5. Statistical Analysis

Our final feature set consisted of 56 features (10 individual, 31 ID/variable ratios, and 15 interaction terms) that made it through one of the three feature screening stages. Predictors used for model development are shown in Table 4. The data was partitioned into 10% testing (n=9) and 90% training (n=86) subsets. A total of 27,720 (56 choose 3) three variable, 367,290 (56 choose 4) four variable, 3,819,816 (56 choose 5) five variable, and 32,468,436 (56 choose 6) six variable linear multivariate models were considered. Bootstrapped average R^2 was calculated from training each model 10 times using

Screened Predictors (56)	
Individual (10)	Dose/var
Cerebellar ROI (CER)	DBP x4
Total Plasma (TotPlas)	MAP x4
Injected Dose (ID)	eCO x3 (pre,post,closest)
HR x3 (pre,post,avg)	PP x3
Weight	CO ₂
BSA	
eTBV	Interaction (15)
eTPV	CER*HR (post,avg)
	Height*COpost
Dose/var (31)	HRpost*TotPlas
Weight	HRpost*Weight
Height	Eosin*DBP (pre,closest)
BMI	MAPclosest*CER
BSA	pH*InjectedMass
LBMI	pH*SpecificActivity
eTBV	RDW*SpecificActivity
eTPV	SpecificActivity ²
eRMR	ThyroxineFree*TotPlas
HR x4 (pre,post,closest,avg)	eTPV*PPpost
SBP x4	Chloride*TotPlas

Table 4: Screened predictors

randomly drawn samples with replacement from the training data and evaluating on the entire training data. Models with the highest average R^2 in each category were applied to the training and test data.

3. RESULTS

Results for top models in terms of average R^2 with and without TP are shown in Table 5. All the models yielded $R^2 > 0.7$. Increasing the number of variables from three to six yielded an R^2 gain of 0.105 and 0.111 with and without TP, respectively. With TP, variables in common were: CER and HR. Other variables present were: BP, eosin, ID, BSA, SpecificActivity and pH. For models without TP, variables in common were: CER, BP, HR, ID, eosin. Other variables present included: Weight, eTBV, and eRMR. It appears that to increase R^2 by 0.1 information about ID and body size is useful. Including TP in model improved R^2 by only 0.015 and 0.009 for the three and six variable model, respectively.

The top six-variable models with and without TP were applied to training and test data. Plots of predicted vs. measured anchor points are shown in Figure 1. Predictions for some points could not be computed due to missing data. With TP in the model, there is a more uniform scattering of points around the identity line and better predictions for the test data. When TP is not included, one test point appears as an outlier possibly due to the fact that TP is very accurately measured via blood sampling on the same day of the PET scan, while all other variables were measured hours to weeks prior.

	Average R^2
Models with Total Plasma variable	
CER + HRavg*CER + HRpost*TotPlas	0.718
CER + HRavg*CER + HRpost*TotPlas + Eosin*BPDiasPre	0.737
CER + HRavg*CER + HRpost*TotPlas + ID/BSA + ID/eRMR	0.796
CER + ID/eRMR + ID/HRpre + TotPlas + Eosin*DBPclosest + pH*SpecificActivity	0.823
Models without Total Plasma variable	
CER + ID/HRpre + Eosin*DBPclosest	0.703
CER + ID/HRpre + Eosin*DBPclosest + ID/COpost	0.714
CER + ID/HRpre + Eosin*DBPclosest + ID/Weight + ID/DBPpost	0.781
CER + ID/HRclosest + Eosin*DBPclosest + ID/eTBV + ID/eRMR + ID/SBPpost	0.814

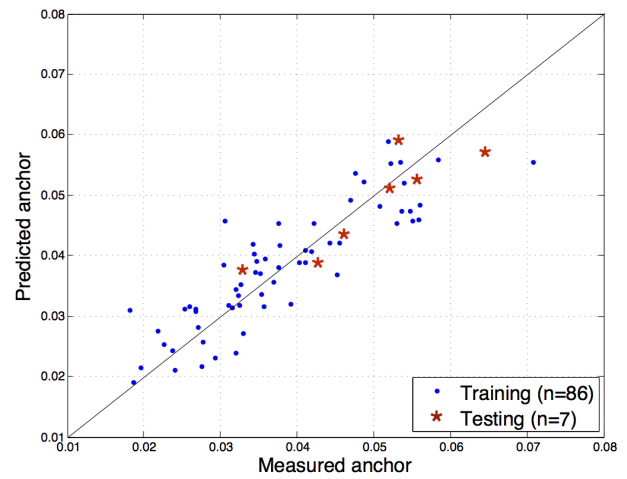
Table 5: Top models with and without Total Plasma

4. CONCLUSIONS

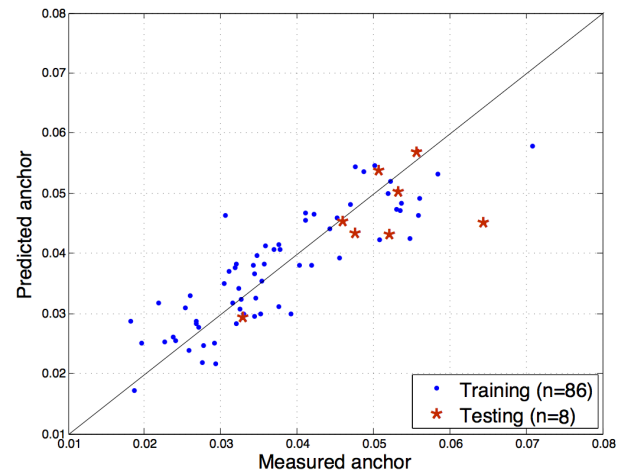
Models for predicting the SIME anchor for $[^{11}\text{C}]\text{DASB}$ were developed using machine learning techniques. Results suggest that $>80\%$ of the variance in $[^{11}\text{C}]\text{DASB}$ metabolism may be explained by variability in HR, BP, ID, body size, and cerebellar gray matter uptake. This is encouraging because this was a retrospective study using data acquired sometimes anywhere from hours (i.e. HR, BP) to weeks (i.e. eosin, pH) from the PET scan date. Furthermore, HR, which appears as an important variable in all the models, was measured via manual radial pulse rate. Weight, a measure on which many other important predictors were based (i.e. eTBV, eRMR, CO) was measured up-to months before the scan. Finally, an extensive evaluation of outliers was not done. Despite these drawbacks, the performance of the models was encouraging and suggests that better predictions of the $[^{11}\text{C}]\text{DASB}$ anchor may be achieved with careful data collection in a prospective study. It is important to recognize the models presented here are the top models in each category in terms of R^2 . Many other models with comparable R^2 are not shown due to space constraints. Evaluation of TP variable, advanced machine-learning techniques, more extensive cross-validation, out-of-sample performance evaluation, and outlier removal is the subject of future work.

5. REFERENCES

- [1] R.B. Innis, V.J. Cunningham, J. Delforge, M. Fujita, A. Gjedde, R.N. Gunn, J. Holden, S. Houle, et al., "Consensus nomenclature for in vivo imaging of reversibly binding radioligands," *Journal of Cerebral Blood Flow & Metabolism*, vol. 27, no. 9, pp. 1533–1539, 2007.
- [2] Ramin V. Parsey, Justine M. Kent, Maria A. Oquendo, Misty C. Richards, Mali Pratap, Thomas B. Cooper, Victoria Arango, and J. John Mann, "Acute occupancy of brain serotonin transporter by sertraline as measured by $[^{11}\text{C}]\text{DASB}$ and positron emission tomography," *Biological Psychiatry*, vol. 59, no. 9, pp. 821–828, May 2006.



(a) With Total Plasma variable



(b) Without Total Plasma variable

Fig. 1: SIME anchor prediction (a) with and (b) without total plasma

- [3] P. Zanotti-Fregonara, R.M. El Mostafa Fadaili, C. Comtat, A. Souloumiac, S. Jan, M.J. Ribeiro, V. Gaura, A. Bar-Hen, R. Tribossen, et al., "Comparison of eight methods for the estimation of the image-derived input function in dynamic ^{18}F -FDG PET human brain studies," *Journal of Cerebral Blood Flow & Metabolism*, vol. 29, no. 11, pp. 1825–1835, 2009.
- [4] R Todd Ogden, Francesca Zanderigo, Stephen Choy, J John Mann, and Ramin V Parsey, "Simultaneous estimation of input functions: an empirical study," *Journal of Cerebral Blood Flow & Metabolism*, vol. 30, no. 4, pp. 816–826, Dec. 2009.
- [5] Eef Hoeben, Martine Neyens, Erik Mannaert, Mark Schmidt, and An Vermeulen, "Population pharmacokinetics of JNJ-37822681, a selective fast-dissociating dopamine d2-receptor antagonist, in healthy subjects and subjects with schizophrenia and dose selection based on simulated d2-receptor occupancy," *Clinical Pharmacokinetics*, vol. 52, no. 11, pp. 1005–1015, June 2013.
- [6] F. O'Sullivan, J. Kirrane, M. Muzi, J. N O'Sullivan, A. M Spence, D. A Mankoff, and K. A Krohn, "Kinetic quantitation of cerebral PET-FDG studies without concurrent blood sampling: Statistical recovery of the arterial input function," *IEEE Transactions on Medical Imaging*, vol. 29, no. 3, pp. 610–624, Mar. 2010.